COPY

AD-A222 725

TITLE: The Validation and Application of a Rotor Acoustic Prediction
Computer Program
*Judith M. Gallman, Mrs.
U. S. Army Aeroflightdynamics Directorate
NASA Ames Research Center
Moffett Field, California 94035

ABSTRACT: A rotor acoustic prediction computer program (RAPP) has been developed to further the understanding of main rotor noise. The prediction program is based on a well known solution to the Ffowcs Willliams and Hawkings equation for acoustic pressure, wherein noncompact monopole terms model rotor blade thickness and distributed dipoles model local blade surface pressure. RAPP has been validated by comparisons with the Boeing model 360 DNW/AATMR acoustic pressure base. This is the first work that utilizes both the acoustic pressure and blade surface pressures acquired during this test. Future applications of RAPP to the study of main rotor noise are discussed.

DTIC
ELECTE
S JUN 0 4 1990
D
D

BIOGRAPHY: Judith M. Gallman
PRESENT ASSIGNMENT: Aerospace Engineer at the U. S. Army Aeroflightdynamics Directorate, 1988-present.
PAST EXPERIENCE: Graduate Scholar Research Assistant at NASA Langley Research Center, 1986-88.
DEGREES HELD: Masters of Science in Aeronautics from The Joint Institute for the Advancement of Flight Sciences, George Washington University/NASA Langley Research Center, 1988. Bachelors of Science in Aerospace Engineering from Parks College of Saint Louis University, 1986.

90 29 133

The Validation and Application of a Rotor Acoustic
Prediction Computer Program

Judith Hoeffner Gallman
U.S. Army Aeroflightdynamics Directorate
NASA Ames Research Center, Mail Stop 215-1
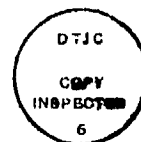Moffett Field, California 94035

Introduction

The rapid development of passive acoustic arrays and signal processing technology that detects, tracks, and identifies a rotorcraft poses a growing threat to the survivability of U. S. combat helicopters. An essential prerequisite to reducing the acoustic detectability of military rotorcraft, and hence to increase their survivability, is a better understanding of main rotor noise, which is the major contributor to the overall noise. A simple, yet accurate, Rotor Acoustic Prediction Program (RAPP) has been developed to advance the understanding of main rotor noise. This prediction program utilizes the Ffowcs Williams and Hawkings (FW-H) equation. The particular form of the FW-H equation[1] used in this analysis is well suited for the coupling of the measured blade surface pressure to the prediction of acoustic pressure.

The FW-H equation is an inhomogeneous wave equation that is valid in all space and governs acoustic pressure generated by thin moving bodies. The nonhomogeneous terms describe mass displacement due to surface motion and forces due to local surface stresses, such as viscous stress and pressure distribution on the surface. There is a rich history of the application of the FW-H equation as applied to the prediction of propeller and rotor noise. The events of the past, which have contributed to the wealth of knowledge in which this paper has its foundation, are discussed in depth in references 1 and 2. The history begins with Gutin's[3] compact source assumption. He modeled steady aerodynamic forces on a propeller with harmonic acoustic dipoles in the frequency domain. Garrick and Watson[4] extended this approach to uniform rectilinear motion. Deming,[5] Arnoldi,[6] and Lyon[7] studied the effects of blade thickness on acoustic noise respectively for static propellers, uniform rectilinear motion, and for helicopters in forward flight. Farassat,[1] Hawkings and Lowson,[8] Isom,[9] and Schmitz and Yu[2] have used noncompact monopole terms to model rotor blade thickness and distributed dipoles to model local blade surface forces.

There are four types of main rotor noise: BVI noise, low-frequency noise, high-speed impulsive noise, and broadband noise.[10] Blade-vortex interaction noise occurs when a tip vortex, previously shed by a rotor blade, passes close enough to a rotor blade to cause large

variations in the blade surface pressures. This event is most disturbing when it happens on the advancing side of the rotor disk.[11] Low-frequency noise includes hover and low to moderate speed forward flight. For these flight conditions, the low frequency components of the acoustic signal dominate. RAPP was developed for BVI and low-frequency applications. These are the flight regimes producing the propagating noise that leads to acoustic detection.

High-speed impulsive noise is a highly nonlinear, transonic phenomenon that is beyond the scope of this work. Recent efforts that do address high-speed impulsive noise couple computational fluid dynamics (CFD) with acoustics. The particular method of Isom and Purcell[12] couples nearfield pressure from a full potential finite-difference method with a Kirchhoff integral formulation to extend the CFD results to the far field. Broadband noise will not be addressed in this paper either. It is of comparatively small amplitude and is a result of unpredictable blade loading such as that caused by turbulence.[13]

RAPP implements the noncompact methods to efficiently and accurately predict BVI noise and low-frequency noise characteristics generated by the main rotor. This paper will explain the details of the blade thickness modeling and the blade surface force modeling used in RAPP. It will establish the validity of RAPP by comparisons with aeroacoustic experimental data for BVI and low-frequency noise. Future applications that are made possible by prediction programs such as RAPP are discussed. The most important application is to use RAPP in conjunction with an aerodynamic blade surface pressure prediction program to learn to design quieter rotor blades. Hence, this would minimize detection ranges and decrease the threat to the survivability of combat helicopters.

Development of the Rotor Acoustic Prediction Program

As stated earlier, RAPP is based on the FW-H equation. This integral equation is expressed as follows:

$$4\pi p'(\vec{x}, t) = \frac{\partial}{\partial t} \int \left[\frac{\rho_0 v_n}{r|1 - M_r|} \right]_{ret} dS(\vec{y})$$

$$+ \frac{1}{a_0} \frac{\partial}{\partial t} \int \left[\frac{p_i \hat{r}_i}{r|1 - M_r|} \right]_{ret} dS(\vec{y}) + \int \left[\frac{p_i \hat{r}_i}{r^2|1 - M_r|} \right]_{ret} dS(\vec{y}) \qquad (1)$$

Equation (1) is an integral equation for the acoustic pressure, p', at a point $\vec{x}$ and a time t. The subscript ret indicates that the integrals are to be evaluated at the retarded time $\tau = t - r/a_0$. The speed of propagation of sound in the fluid medium is designated by a_0, and ρ_0 is the density of the undisturbed fluid medium. M_r is the Mach number in the radiation direction, $M_r = \frac{V_i \hat{r}_i}{a_0}$. In this equation for the radiation Mach number, V_i is the local free stream velocity vector, and $\hat{r}_i$ is the unit vector describing the radiation direction. For the above form of equation (1), the radiation Mach number should not equal 1. As a rule, the advancing tip Mach number should remain below the critical Mach number for the airfoil section. RAPP does not contain any nonlinear terms and should not be applied to nonlinear circumstances such as the transonic flow regimes.

The first term on the right-hand side of equation (1) is referred to as the thickness term. This term represents the disturbance of the fluid medium caused by the airfoil. For a fixed volume, a short fat airfoil will cause a greater displacement than a long slender airfoil. This is the influence of the normal velocity on the airfoil surface. Thin airfoil theory defines the normal velocity as

$$v_n = V_0 [\alpha + \tan^{-1} \frac{dy}{dx}] \tag{2}$$

Here α is the airfoil angle of attack, V_0 is the local freestream velocity, and $\frac{dy}{dx}$ is the thickness distribution of the airfoil. Even though the angle of attack is not zero, the term

$$\frac{\partial}{\partial t} \int \frac{\rho_0 V_0 \alpha}{r(1 - M_r)} dS(\vec{y}) \tag{3}$$

is negligible. It does not contribute to the thickness noise, even for $\alpha \geq 10°$, and has been neglected by other researchers, namely Schmitz and Yu[2]. The term

$$\frac{\partial}{\partial t} \int \frac{\rho_0 V_0 \frac{dy}{dx}}{r(1 - M_r)} dS(\vec{y}) \tag{4}$$

can be approximated quite well by a chordwise distribution of sources and sinks at about five spanwise locations. The sources are assumed to be of strength

$$ss = \rho_0 V_0 \frac{dy}{dx} \tag{5}$$

Equation (4) can be discretized as

$$\rho_0 \frac{\partial}{\partial t} \sum_{i=1}^{n} \sum_{j=1}^{m} \frac{V_{0_{ij}} dy_{ij}}{r_{ij}(1 - M_{r_{ij}})} dz_i \tag{6}$$

Here $dS = dx\,dz$, and the subscript ij indicates quantities that are functions of both the chordwise and spanwise variables. The thickness of the airfoil at the ith spanwise location and the jth chordwise location is dy_{ij}. The thickness noise has been well modelled with 10 chordwise sources at each of 5 spanwise radial stations. Adding more sources and more stations does not improve the accuracy of the thickness prediction. It just takes more computational time. This was verified by adding more radial stations and more sources at these radial stations to RAPP in the developmental stage.

The second and third terms in equation (1) are the loading terms. Only the second term in equation (1) will be used to predict the loading noise for two reasons. The third term, which does not include a partial time derivative, is considered the near-field term. It is divided by the square of the distance between the source and the observer. For an observer in the far-field, this near-field term is negligible. Also, the quasi-steady near-field

acoustic pressure was not measured by the microphones used in acquiring acoustic test data. These microphones were back vented free-field response microphones. Consequently the frequency of the quasi-steady near-field acoustic pressure was below the low frequency response of these microphones.

RAPP uses the acoustic lifting line formulation to model the loading noise. If the loading information is supplied as blade surface pressure, the sectional lift and drag are determined by integrating the surface pressure over the chord. The loading term can be discretized as follows:

$$\frac{1}{a_0}\frac{\partial}{\partial t}\sum_{i=1}^{m} c_i \left[\frac{l\hat{n}_l \cdot \hat{r} + d\hat{n}_d \cdot \hat{r}}{r(1 - M_r)}\right]_i dz_i \tag{7}$$

The sectional lift and drag are defined by l and d. The normal vectors $\hat{n}_l$ and $\hat{n}_d$ are defined parallel and perpendicular to the tip path plane of the rotor. The airfoil is exerting a force on the fluid, therefore, convention defines lift as positive downward and drag as positive toward the leading edge of the airfoil. Figure (1) displays the sign convention of these normal vectors in the blade fixed coordinate system. Two important assumptions that have been made in arriving at equation (7) are that the distance r and the radiation Mach number M_r are held constant over the chord, c_i. The loading terms are modelled well by equation (7) with five radial stations on the outer 50 percent of the rotor span.
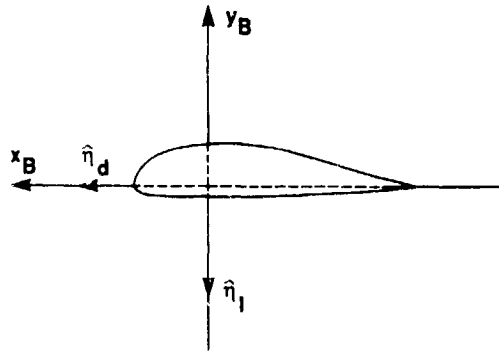

Figure 1. Presentation of the sign convention for the surface normals in the blade fixed coordinate system.

The thickness and loading terms must be evaluated at the retarded time, τ. This allows for the proper summation of the acoustic disturbances at the observer location and time. An iterative technique is needed to solve for the location of all the sources that contribute to the acoustic disturbance for a time t and observer $\bar{x}$. Iteration is necessary to solve the retarded time equation because the distance between the source and the observer is a function of the source time. The locations of the contributing sources comprise the acoustic planform. The acoustic planform is defined as the locus of emitting source locations whose signals arrive simultaneously at a time t to the observer. Please note that the surface over which

the integration is carried out is not the acoustic planform, but rather the physical geometric planform.

Both the Newton iteration method and the Bisection method are used to solve for the source locations on the acoustic planform. Newton's method converges quickly, or in just a few function evaluations, if the initial guess is "close enough" to the solution. Although the function on which the iterations are being performed,

$$f(x) = t - (\tau - \triangle\tau + r(\tau - \triangle\tau)/a_0) \tag{8}$$

is a continuously increasing function, $f'(x)$ can become very small. Since this term is the denominator in the iteration scheme, the method will not converge unless the initial guess is close enough to the solution. To guarantee convergence of Newton's method, a satisfactory initial guess is supplied by the Bisection method. This method is not affected by $f'(x)$, but it does require many function evaluations. This is why Newton's method is used to conclude the iteration after the Bisection method finds a suitable first guess.

A central difference method, which is second-order accurate, is used for the time derivative. The time derivatives of the thickness and loading terms are taken separately, so that the contribution to the acoustic disturbance from each phenomenon can be studied separately.

Validation of the Prediction Code

Discussion of Test Data

RAPP was validated by comparisons with the Boeing 360 experimental acoustic test data acquired during the Aerodynamic and Acoustic Testing of Model Rotors (AATMR) program at the Duits-Nederlandse Windtunnel (DNW). The DNW Boeing 360 model rotor acoustic database has been reviewed and analyzed by Zinner et al.,[10] and is considered of high quality to validate acoustic prediction codes. Zinner shows that the Boeing 360 acoustic test data displays the expected trends for high-speed impulsive noise, blade-vortex interaction noise, low-frequency noise, and broadband noise. The conditions for maximum BVI noise were shown to range from low shaft-tilt angles at high advance ratios to high shaft-tilt angles at low advance ratios. BVI noise has maximum radiation in the direction toward the advancing side of the rotor and at least 25 degrees below the rotor plane. A severe test of RAPP's predictive ability will be whether or not it can predict these trends for BVI.

The accuracy of RAPP's predictive ability depends on the accuracy of the input blade surface pressure. The DNW Boeing 360 experimental surface pressure data has been utilized by Caradonna et al[14] in the prediction of airloads and is considered to be of the quality necessary to support test/theory. Thus, this DNW Boeing 360 blade surface pressure was thought to be a good source of input to validate RAPP. Both Caradonna and Zinner have discussed the DNW test facility, the data acquisition system, and the characteristics of the model rotor in great detail. The interested reader should study references 10 and 14 for more information on this experiment.

The sectional lift and drag, supplied as input for RAPP, were obtained by integrating the Boeing 360 surface pressure over the chord. This technique did not work well for the

hover flight regime since drag dominates the loading noise contribution. There are an insuf ficient number of pressure taps to get an accurate estimate of the sectional drag. Analytical estimates of the sectional drag are better suited for this application and are easy to determine for hover where the loading is ideally constant about the azimuth. A good source of the sectional lift and drag is a potential flow lifting surface analysis program, such as that by Analytical Methods Incorporated (AMI).[15] The sectional lift and drag from AMI's hover code was used in RAPP to predict the helicopter noise in hover. For the forward and descending flight regimes, the DNW Boeing experimental surface pressure data was used as input. The technique of integrating the surface pressure chordwise to get the sectional lift and drag worked well for these flight regimes because the lift dominates the loading noise contribution.

Figure 2 shows the microphone array that was used to acquire test data. These microphone locations define the observer positions. This array of microphones is located a distance of three rotor radii from the rotor hub.
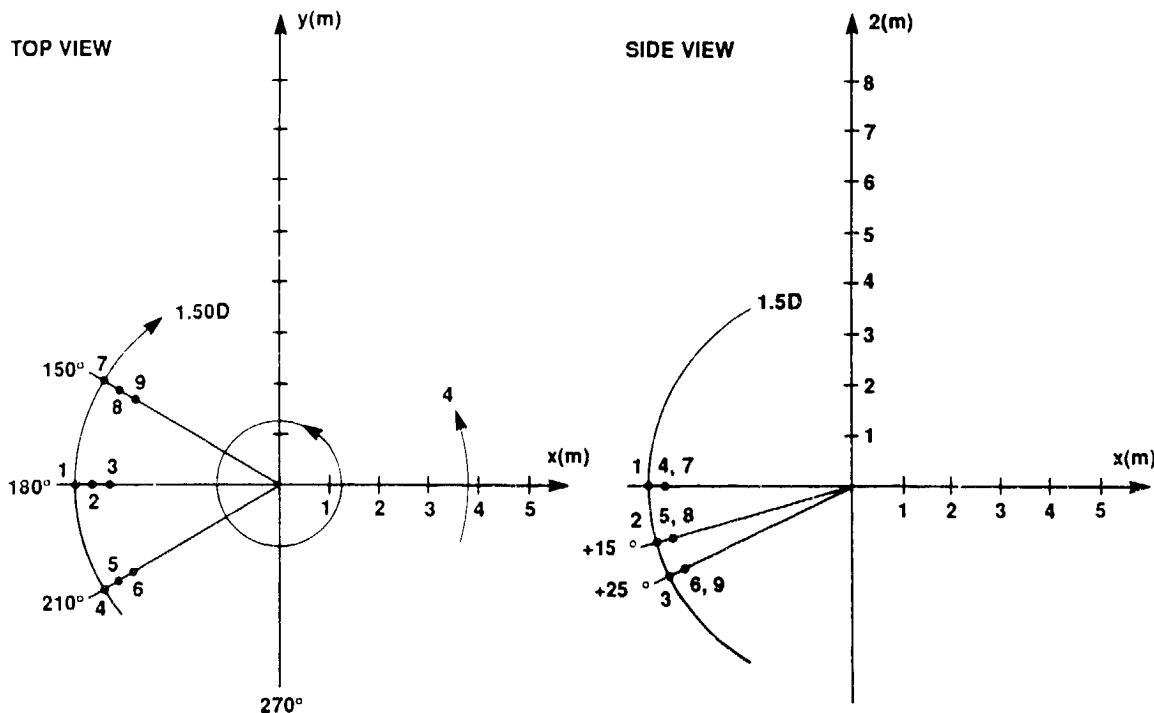

Figure 2. Microphone array used to acquire acoustic pressure for the Boeing model 360 DNW/AATMR test

RAPP was first applied to predict acoustic pressure in the hover flight regime. Since the loading is ideally constant around the azimuth for the hovering rotor, it was a natural first step in the developmental process. Five hover test points were chosen from the Boeing 360 data base for the hover comparisons. All five test points had the same solidity weighted thrust coefficient $C_T/\sigma = .07$, with hover tip Mach number ranging from $M_H = .5$ to $M_H = .636$. The loading, or the sectional lift and drag, from the AMI Hover code supplied input to RAPP to match these five test conditions. In Figure 3a, the plots of predicted peak negative pressure versus Mach number depict the trend for hover of decreasing peak negative pressure below the rotor tip path plane. The peak negative pressure is defined as the most negative peak amplitude in the acoustic pressure time histories At this loading condition, the thickness noise is dominant and its amplitude decreases below the tip path plane. The loading noise, which becomes predominant below the plane, does not increase more than the thickness decreases. Predicted peak negative pressure versus Mach number plots are compared to the measured plots of peak negative pressure versus Mach number in figures 3b, 3c, and 3d. Figure 3b shows comparisons for the in-plane microphone, $\phi = 0°$. The comparisons for the in-plane microphone are quite acceptable. Figure 3c shows comparisons for the microphone at $\phi = 15°$ below the tip path plane, and figure 3d shows comparisons for the microphone at $\phi = 25°$ below the tip path plane. The comparisons in figures 3c and 3d are not acceptable. The experimental plots do not display the expected trend of decreasing below the tip path plane. This is due to recirculation of the air in the DNW test chamber. The DNW is not a hover chamber and does not allow for clean hover test conditions. A mean flow and recirculation occur in the test chamber and cause unsteady effects in the loading and in the acoustics. These unsteady affects are most noticeable in the out-of-plane observer locations and are quite noticeable in the plots shown in figures 3c and 3d. However, the in-plane comparisons, as shown in figure 3a, are good enough to conclude that RAPP can accurately predict acoustic pressure for the hover flight regime.

The next step in the development of RAPP was to predict acoustic pressure in forward flight and in descent where BVI occurs. In these flight regimes, RAPP will have to contend with blade loading that varies about the azimuth. To get an accurate prediction, the blade loading must be known at many locations around the azimuth. The measured experimental pressure is known at 1024 locations around the azimuth. This resolution of almost every one-third of a degree enables the acoustic prediction program to compute accurate pressure time histories. Computer programs that calculate blade surface pressure for forward flight and BVI flight regimes are beginning to have the ability to predict the blade loading at very fine increments in azimuthal angle. The application of this capability to the Boeing 360 rotor will be discussed in the application section of this paper.

To validate RAPP for the forward and descending flight regimes, the measured surface pressure data from the Boeing 360 model rotor test was used as input. The surface pressure was integrated over the chord to get the sectional lift and drag at each radial station and azimuth angle. The acoustic pressure time histories, predicted using the experimental surface pressures as input to RAPP, compare well with the measured acoustic pressure time histories. This is presented in figures 4 and 5 which show comparisons of predicted to measured acoustic pressure time histories. Figure 4a shows the in-plane comparisons for a moderately high speed forward flight test point. Figure 4b shows comparisons for observers 25° below
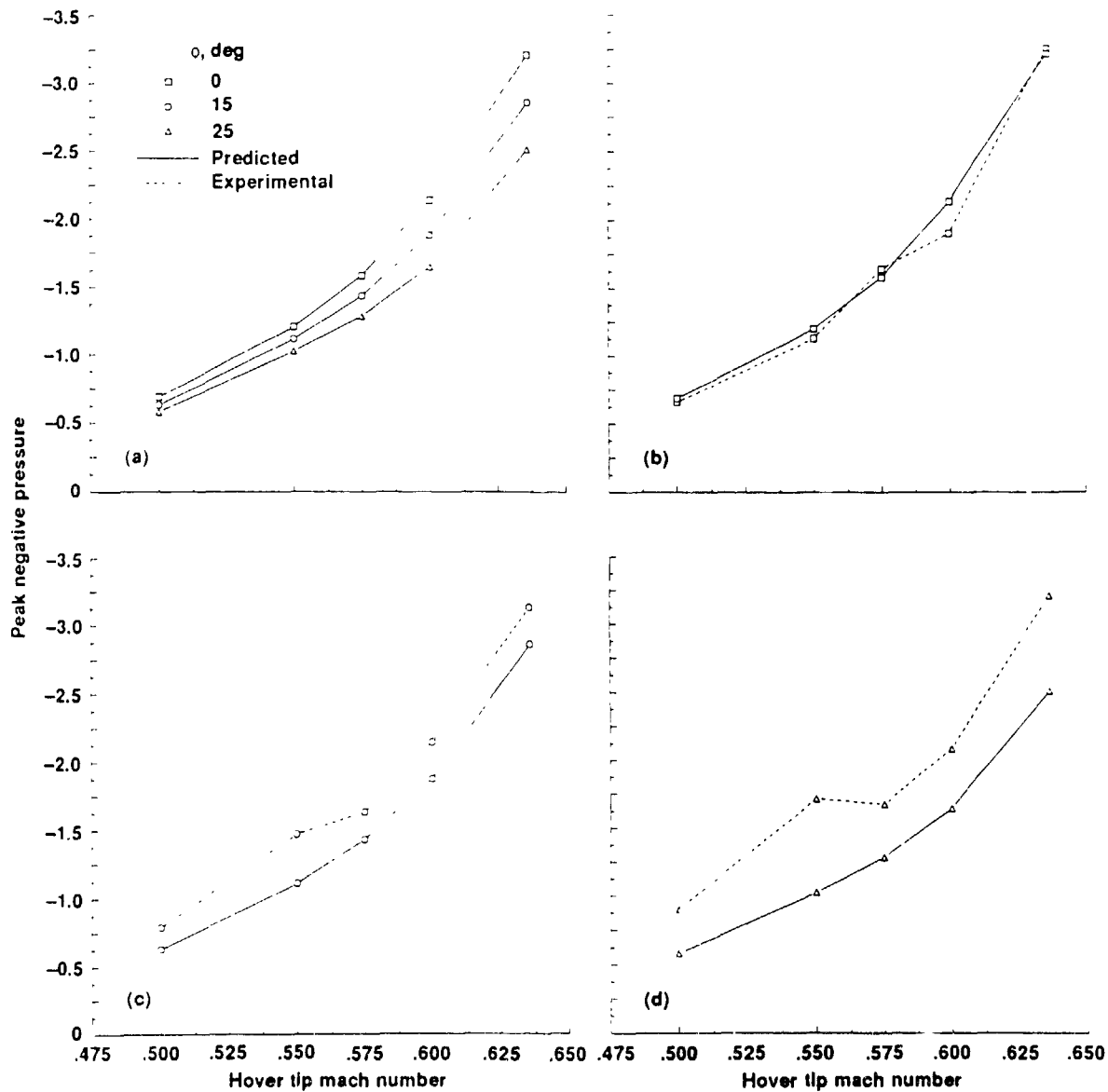
Figure 3. Plots of peak negative acoustic pressure versus mach number. (a) Depicts predicted trends. (b) Shows comparisons for inplane microphones, o = 0. (c) Shows comparisons for microphones at φ = 15° below the ti, path plane. (d) Shows comparisons for microphones at φ = 25° below the tip path plane.

the tip path plane for this same test point. Figure 5a shows the in-plane comparisons for a descent or BVI test point. Figure 5b shows comparisons for observers 25° below the rotor plane. This data for BVI portrays the expected trends where the highest peak-to-peak levels
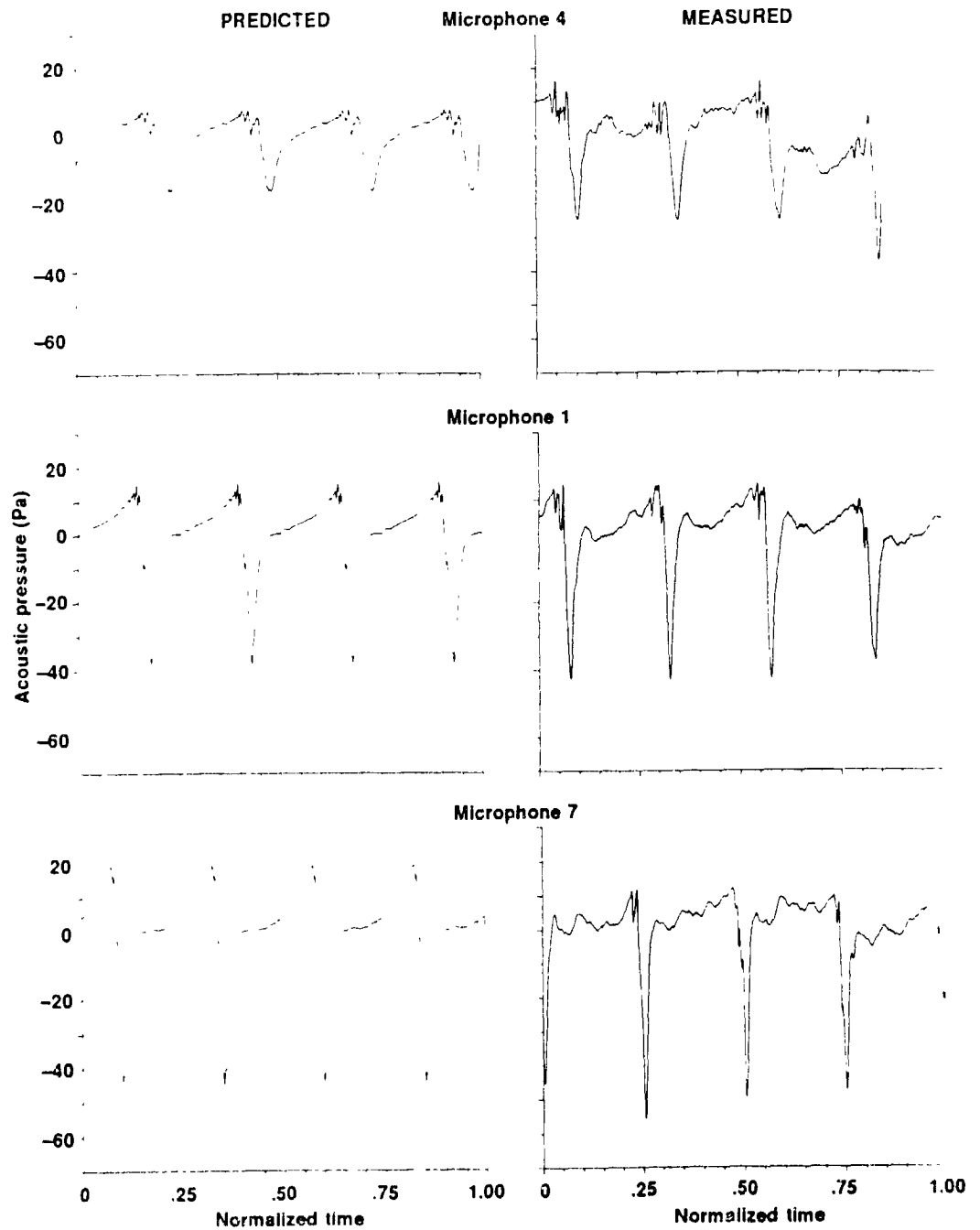
Figure 4a. Plots of acoustic pressure time histories for microphones in the up path plane. The flight conditions are $\mu = 0.356$, $CT/\alpha = 0.07$, and shaft tilt $= -5.55°$.
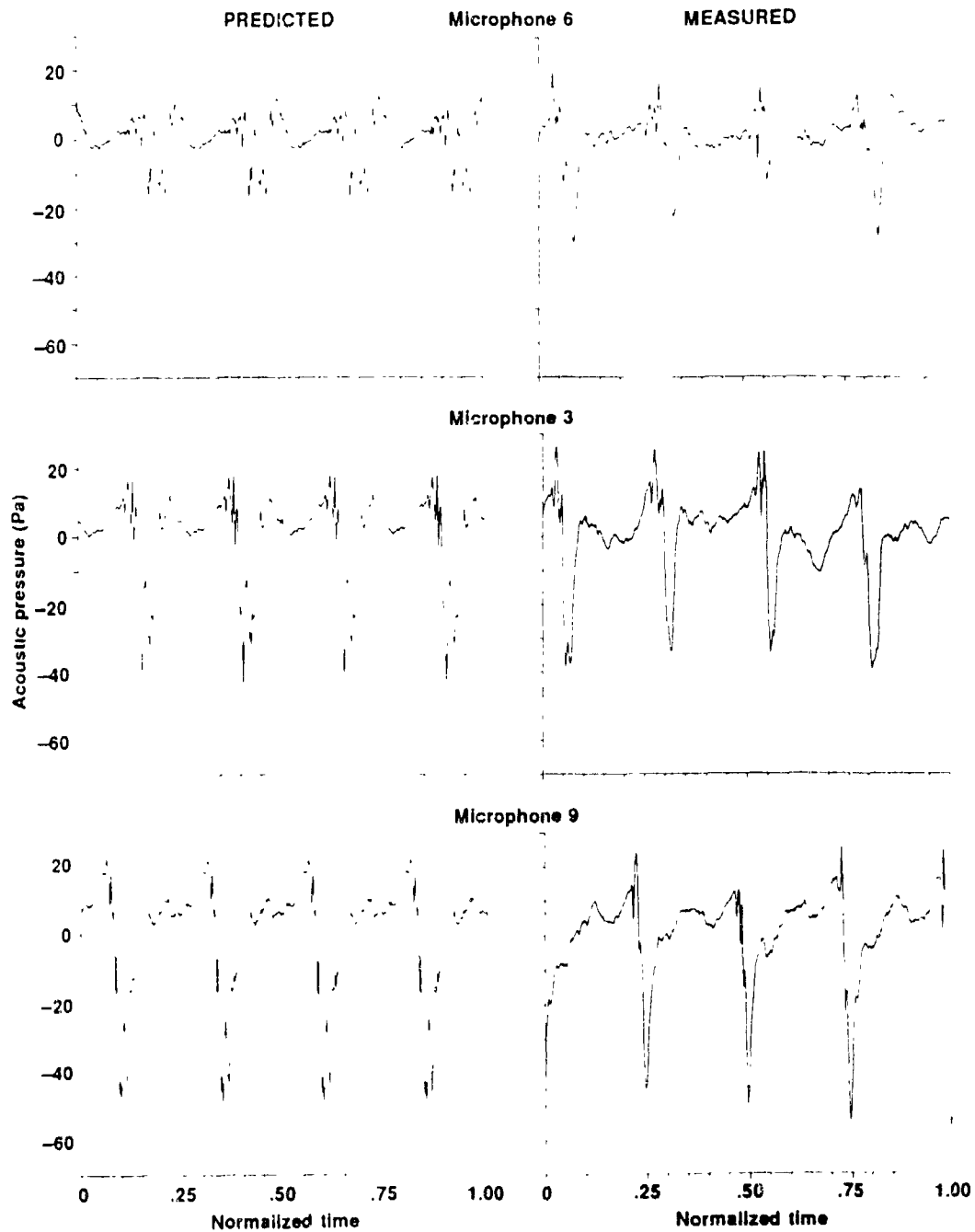
Figure 4b. Plots of acoustic pressure time histories for microphones 25° below the up path plane. The flight conditions are $\mu = 0.356$, $CT/\alpha = 0.07$, and shaft tilt = 5.55°
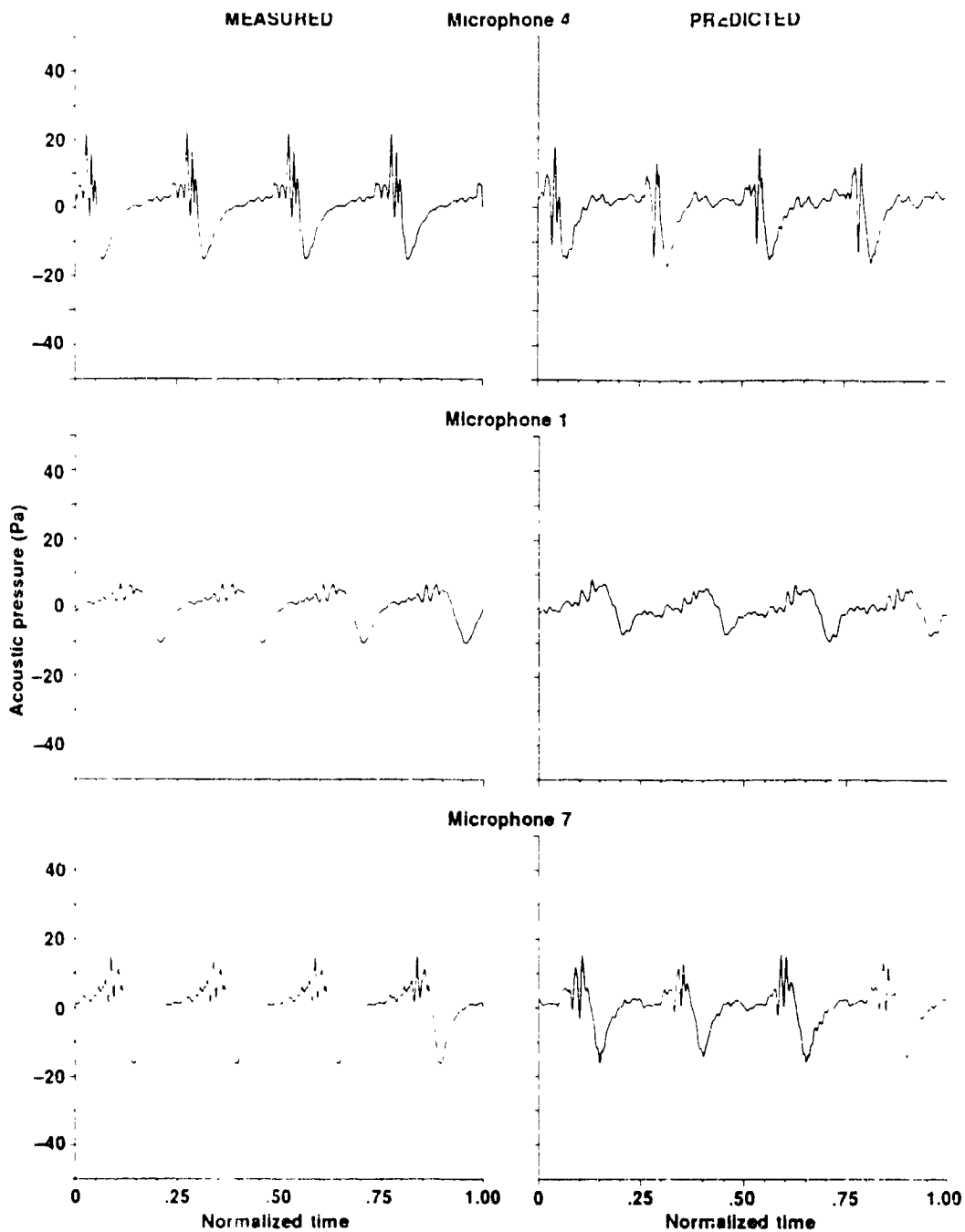
Figure 5a. Plots of acoustic pressure time histories for microphones in the up path plane. The flight conditions are $\mu = 0.225$, $CT/\alpha = 0.07$, and shaft tilt = 4.38°
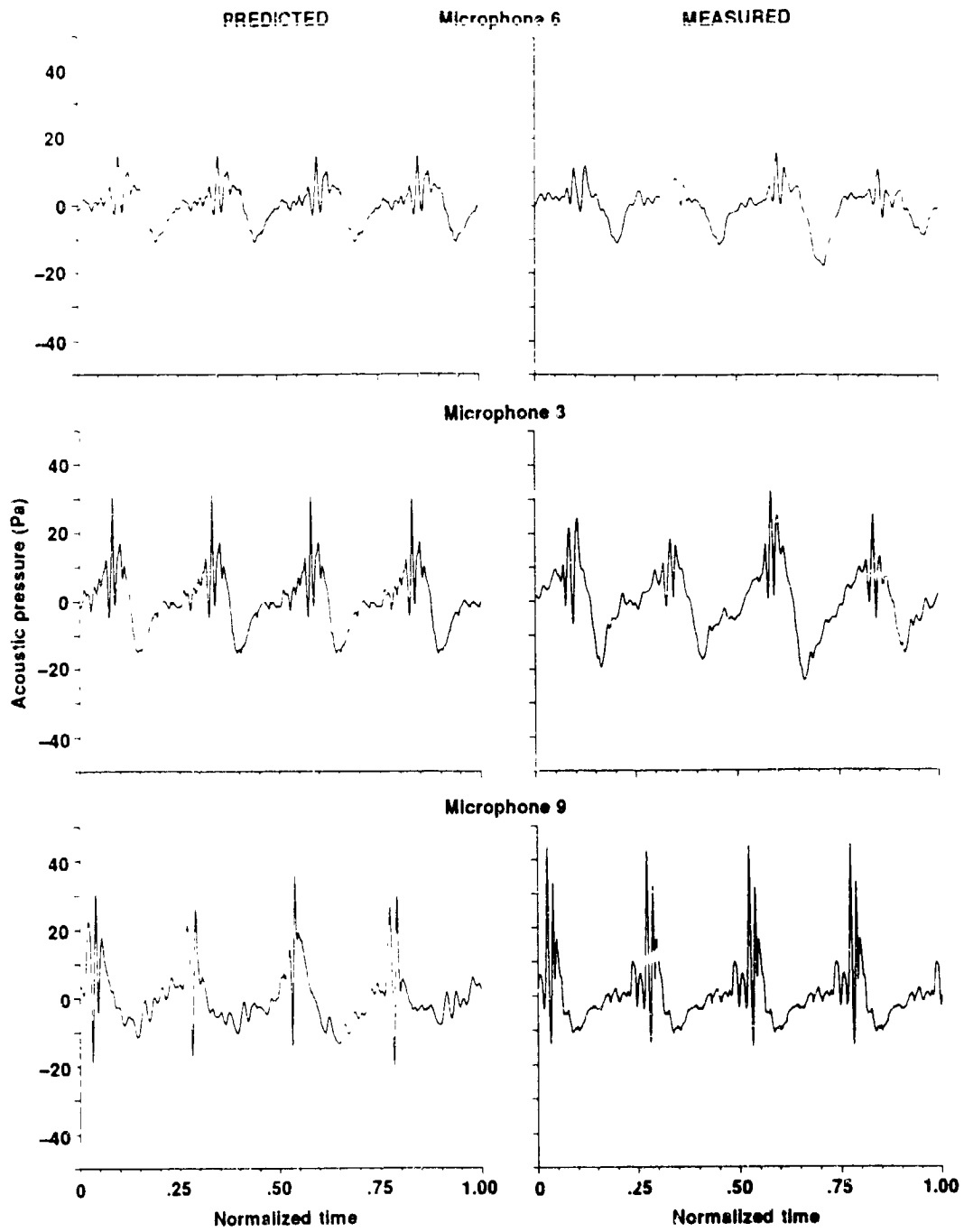
Figure 5b. Plots of acoustic pressure time histories for microphones 25° below the tip path plane. The flight conditions are $\mu = 0.225$, $CT/\alpha = 0.07$, and shaft tilt = 4.38°.

are near 150° azimuth and 25° below the plane. It can be concluded from the comparison plots in figures 4 and 5 that RAPP is capable of predicting accurate acoustic pressure time histories for moderate-speed forward flight and BVI.

Applications

A prediction program such as RAPP, can be applied to study many aspects of main rotor noise. The contribution of the three noise generating mechanisms— thickness, lift, and drag— to the total acoustic pressure disturbance can be plotted separately. This allows for a more in-depth study of each noise generating mechanism. An example of such a plot is shown in figure 6 for an in-plane microphone from the same forward flight test point shown in figure 4a.

The prediction of acoustic pressure is dependent upon the knowledge of the blade loading. Reliable sources of predicted blade loading are becoming available as the research in blade surface pressure prediction progresses. The most promising technique developing is the coupling of a full-potential rotor flow solver with a comprehensive lifting surface analysis. It is becoming possible for the techniques to produce the surface pressure at the number of azimuthal angles necessary for accurate acoustic prediction for forward flight and BVI. A very fine resolution in azimuth angle is necessary for accurate BVI predictions because the surface pressure changes so abruptly in a short source time increment. Possible future applications for RAPP are to use the blade surface prediction capabilities to study the effects of varying airfoil sections, twist distributions and planform shape on BVI. This application could lead to helicopter rotor systems that are designed to be quieter in the BVI flight regime.

Another application of RAPP, when used in conjunction with blade surface pressure prediction codes, is to predict experimental wind tunnel test data before the test is run. This would allow the experimentalist to decide the best microphone specifications and locations and at which test conditions to run. These predictions of the test data could help the experimentalist decide on the integrity of the data being acquired. The overall effect would be better planned wind tunnel tests that would provide more useful data.

Conclusions

The most important conclusion that can be drawn from the information presented in this paper is that RAPP can predict accurate rotor acoustic pressure time histories. The notable technique and assumption used in RAPP is the acoustic lifting line formulation. This formulation works well and considerably simplifies the application of the FW-H equation. RAPP is a simple enough program to run on a personal computer and executes in RAPidly. Therefore, the above mentioned applications could take place in the test field or in an industrial setting where supercomputers are not the norm.

Some interesting byproducts of RAPP's developmental process concern the details of the computer program. Details such as 10 sources along the chord at 5 radial stations being necessary and sufficient to accurately predict thickness noise. It is also interesting that even BVI noise can be predicted accurately by modeling the loading terms at only 5 radial stations. This indicates that the azimuthal resolution is more important than the
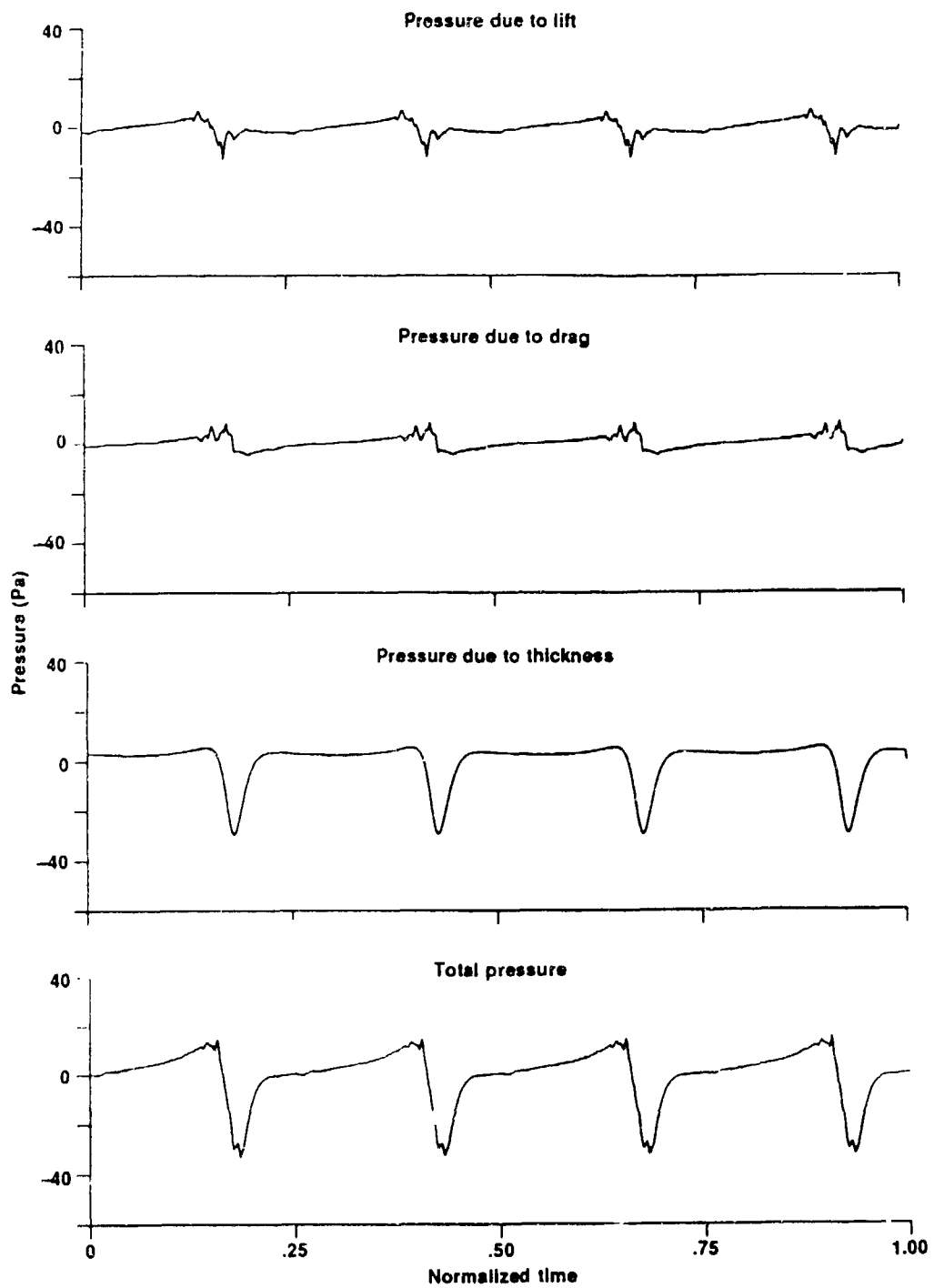
Figure 6. The contributions of the noise generated by lift, drag and thickness are plotted separately.

spanwise resolution. The fact that the acoustic predictions for hover rely so heavily on accurate section drag input will prove useful in future hover acoustic predictions.

References

[1] F. Farassat, Theory of ` ise Generated From Moving Bodies with an Application to Helicopter Rotors, *NASA Th   452*, Dec. 1965.

[2] F. Schmitz, Y. H. Yu, Theoretical Modeling of High Speed Helicopter Impulsive Noise, Presented at The 3rd European Rotorcraft and Powered Lift Aircraft Forum, Aux-En-Provence, France, Sept. 1977.

[3] L. Gutin, On the Sound Field of a Rotating Propeller, *Physik. Zeitschr. der Sowjetunion*, Bd. 9, Heft 1, 1936, pp. 57-71. Trans. *NACA TM 1195*, 1948.

[4] I. E. Garrick, C. E. Watkins, A Theoretical Study of the Effect of Forward Speed on the Free-Space Sound Pressure Field Around Propellers, *NACA Report 1198*, 1954.

[5] A. F. Deming, Noise from Propellers with Symmetrical Sections at Zero Angle, *NACA TN 679*, 1938.

[6] R. A. Arnoldi, Propeller Noise Caused by Blade Thickness, Rep. R-08961, Res. Dep., United Aircraft Corp., Jan. 10, 1956.

[7] R. H. Lyon, Radiation of Sound by Airfoils that Accelerate Near the Speed of Sound, *J. Acoustical Society of America*, Vol. 49, No. 3, March 1971, pp. 894-905.

[8] D. L. Hawkings, M. V. Lowson, Theory of Open Supersonic Rotor Noise, *J. Sound and Vibration*, Vol. 36, No. 1, Sept. 1974, pp. 1-20.

[9] M. P. Isom, The Theory of Sound Radiated by a Hovering Transonic Helicopter Blade, Poly-AE/Am. Rep. No.75-4. Department of Aerospace Engineering and Applied Mechanics, Polytechnic Institute of New York, May 1975.

[10] R. A. Zinner, et al., Review and Analysis of the DNW/Model 360 Rotor Acoustic Data Base, Presented at The 15th European Rotorcraft Forum, Amsterdam, Netherlands, Sept. 1989.

[11] F. H. Schmitz, Y. H. Yu, Helicopter Impulsive Noise: Theoretical and Experimental Status, *J. Sound and Vibration*, Vol. 109, 1986, pp. 361-422.

[12] M. Isom, T. Purcell, R. Strawn, Geometrical Acoustics and Transonic Helicopter Sound, Presented at the AIAA 11th Aeroacoustics Conference, Sunnyvale, California, Oct. 1987.

[13] T. F. Brooks, et al., Main Rotor Broadband Noise Study in the DNW, AHS Aerodynamics and Aeroacoustics Specialists Meeting, 198/.

[14] L. Dadone, F. Caradonna, et al., The Prediction of Loads on the Boeing Helicopter's Model 360 Rotor, Presented at The 45th Annual Forum and Technical Display of the American Helicopter Society, Boston, May 1989.

[15] J. M. Summa, B. Maskew, A Surface Singularity Method for Rotors in Hover or Climb, *USAAVRADCOM TR 81-D-23*, December 1981.